

Elastocaloric effect of Ni-Ti wire for application in a cooling device

J. Tušek, K. Engelbrecht, L. P. Mikkelsen, and N. Pryds

Citation: *Journal of Applied Physics* **117**, 124901 (2015); doi: 10.1063/1.4913878

View online: <http://dx.doi.org/10.1063/1.4913878>

View Table of Contents: <http://scitation.aip.org/content/aip/journal/jap/117/12?ver=pdfcov>

Published by the [AIP Publishing](#)

Articles you may be interested in

[Structural transformations in NiTi shape memory alloy nanowires](#)

J. Appl. Phys. **115**, 194307 (2014); 10.1063/1.4876715

[Stress-induced transformations at low temperatures in a Ni₄₅Co₅Mn₃₆In₁₄ metamagnetic shape memory alloy](#)

Appl. Phys. Lett. **103**, 242406 (2013); 10.1063/1.4840336

[Stress-induced transformation behaviors at low temperatures in Ti-51.8Ni \(at. %\) shape memory alloy](#)

Appl. Phys. Lett. **102**, 231915 (2013); 10.1063/1.4809935

[Demonstration of high efficiency elastocaloric cooling with large \$\Delta T\$ using NiTi wires](#)

Appl. Phys. Lett. **101**, 073904 (2012); 10.1063/1.4746257


[Neutron diffraction investigation of hysteresis reduction and increase in linearity in the stress-strain response of superelastic NiTi](#)

Appl. Phys. Lett. **88**, 201919 (2006); 10.1063/1.2204650


A promotional banner for the Journal of Applied Physics. It features the AIP logo and the text 'Journal of Applied Physics' at the top. Below this, it says 'Meet The New Deputy Editors'. Three circular portraits of the new deputy editors are shown: Christian Brosseau, Laurie McNeil, and Simon Phillpot, each with their name written below their portrait.

AIP | Journal of Applied Physics

Meet The New Deputy Editors

 Christian Brosseau

 Laurie McNeil

 Simon Phillpot

Elastocaloric effect of Ni-Ti wire for application in a cooling device

J. Tušek,^{1,a)} K. Engelbrecht,¹ L. P. Mikkelsen,² and N. Pryds¹

¹Department of Energy Conversion and Storage, Technical University of Denmark (DTU), Risø Campus, Frederiksborgvej 399, DK-4000 Roskilde, Denmark

²Department of Wind Energy, Technical University of Denmark (DTU), Risø Campus, Frederiksborgvej 399, DK-4000 Roskilde, Denmark

(Received 28 November 2014; accepted 17 February 2015; published online 24 March 2015)

We report on the elastocaloric effect of a superelastic Ni-Ti wire to be used in a cooling device. Initially, each evaluated wire was subjected to 400 loading/unloading training cycles in order to stabilize its superelastic behavior. The wires were trained at different temperatures, which lead to different stabilized superelastic behaviors. The stabilized (trained) wires were further tested isothermally (at low strain-rate) and adiabatically (at high strain-rate) at different temperatures (from 312 K to 342 K). We studied the impact of the training temperature and resulting superelastic behavior on the adiabatic temperature changes. The largest measured adiabatic temperature change during loading was 25 K with a corresponding 21 K change during unloading (at 322 K). A special focus was put on the irreversibilities in the adiabatic temperature changes between loading and unloading. It was shown that there are two sources of the temperature irreversibilities: the hysteresis (and related entropy generation) and the temporary residual strain immediately after unloading, respectively. The latter results in the temporary bending of the wire and reduced negative adiabatic temperature change. The paper also shows the impact of the applied strain on the adiabatic temperature changes as well as the distribution of the elastocaloric effect over the wire during loading in the case of two wires trained at different temperatures and the virgin wire, respectively. In the end, we propose guidelines about the required material properties for an efficient elastocaloric cooling device. © 2015 AIP Publishing LLC. [<http://dx.doi.org/10.1063/1.4913878>]

I. INTRODUCTION

Solid materials can change their temperature when subjected to a sudden change of an external field such as magnetic (magnetocaloric effect), electric (electrocaloric effect), mechanical stress (elastocaloric effect), or hydrostatic pressure (barocaloric effect). These properties are in general known as the caloric effects¹ and are related to a change in the material's entropy and/or temperature when an external field is applied. A large effort nowadays is devoted to investigating solid-state refrigeration using the magnetocaloric effect (change of temperature upon application of a magnetic field)—see Refs. 2–4. However, the possibility of inducing a thermodynamic transition by means of mechanical stress, i.e., the elastocaloric effect (eCE) in superelastic materials, opens up new routes for solid-state refrigeration.

The eCE is observed as the entropy change under isothermal conditions or temperature change under adiabatic conditions when a mechanical stress is applied or released in a given material. This is directly related to the phenomenon of reversible solid-to-solid martensitic phase transformation.⁵ Martensitic transformation (i.e., from austenite to martensite) is a first-order diffusionless structural transformation, which can be induced by reducing the temperature or by applying an external stress. The reverse transformation takes place by heating from the martensitic state or by releasing the stress, which also restores the original shape of the particular material. This effect is also known as the shape-memory effect (temperature-induced transformation) or superelastic effect

(stress-induced transformation). In order to generate the eCE, the stress-induced transformation is required. When stress is applied to the elastocaloric (superelastic) material, the exothermic austenitic-martensitic transformation occurs. If that happens fast enough, the material heats up. For some materials, the released latent heat can be as high as 20 J/g.⁶ Upon stress removal, the reverse endothermic martensitic-austenitic transformation occurs, the material cools down, and heat can be absorbed from the surroundings. This process (as a cooling cycle) is schematically shown in Fig. 1.

The first shape memory and superelastic effect were observed in the 1930s in Au-Cd and later in a Cu-Zn alloy.⁷ However, so-far the most widely used and analyzed

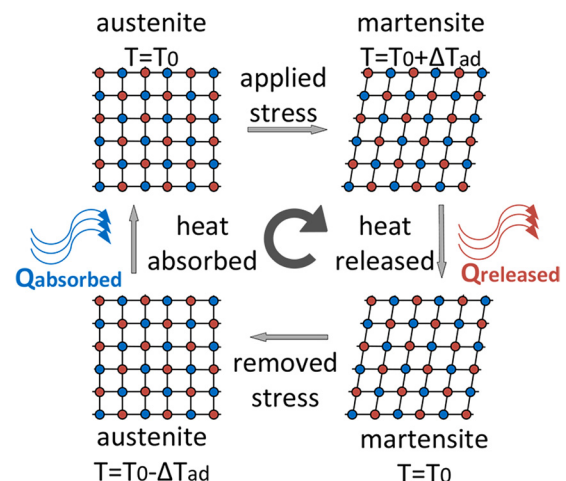


FIG. 1. A schematic show of the elastocaloric cooling cycle.

^{a)}E-mail: jatu@dtu.dk

shape-memory and superelastic alloy is near-equiatomic Ni-Ti alloy first presented in 1963. In the later years, a number of shape-memory and superelastic alloys were developed and characterized;⁷ e.g., Ni-Ti alloys (doped with Cu, Co, Pd, etc.); Cu-based (doped with Al, Ni, Zn, Mn, etc.), and Fe-based (doped with Pd, Mn, Si, Ni, etc.). The shape memory and superelastic effects are also exhibited by polymers, although not caused by the martensitic transformation (see Ref. 8).

As explained by Moya *et al.*,⁹ the eCE was first detected already in early 19th century in Indian rubber by rapidly stretching and releasing it. Some fifty years later Joule reported modest temperature changes (≈ 0.2 K) caused by reversible elastic heat in some metals and dry woods.⁹ However, the first studies on the latent heat and related temperature changes in superelastic materials at room temperature were performed in the 1980s, mostly in Ni-Ti and Cu-based alloys,^{10–13} while more recent studies can be found in Refs. 14–16. Those studies were not focused on properties relevant to refrigeration or heat-pumping purposes, but rather on the strain-rate impact and the origin of these thermal effects. In 1992, Nikitin *et al.*¹⁷ published the eCE in Fe-Rh alloy near room temperature. They measured a negative adiabatic temperature change of 5.2 K (and indirectly, using the Clausius-Clapeyron equation, estimated a change of 8.7 K) under the stress removal of 529 MPa at 305 K. In 2008, Bonnot *et al.*¹⁸ analyzed the eCE of single-crystalline Cu-Zn-Al alloy and estimated its adiabatic temperature change of 15 K when they applied a mechanical stress of 28.5 MPa at 300 K (by Clausius-Clapeyron equation). In recent years, the eCE of this alloy was further analyzed by Vives *et al.*¹⁹ and Manosa *et al.*,²⁰ who measured a negative adiabatic temperature of about 6 K in a temperature range between 200 and 350 K under the removal of the applied stress up to 275 MPa. Cui *et al.*⁵ analyzed the eCE of poly-crystalline Ni-Ti wires at room temperature (295 K) and measured an adiabatic temperature change of 25.5 K when they applied a stress of 650 MPa and -17 K when the stress was removed. Similarly, Ossmer *et al.*^{21,22} analyzed the eCE in Ni-Ti thin film and measured a positive adiabatic temperature change of 17 K and negative of 16 K. Bechtold *et al.*²³ compared the eCE and functional stability of Ni-Ti and Ni-Ti-Cu thin films. They concluded that adding Cu to the Ni-Ti alloy results in more stabilized superelastic behavior and, therefore, potentially better fatigue life than an undoped sample, but the doping also increased transformation temperatures significantly above room temperature. In 2013, Xiao *et al.*²⁴ reported the eCE of single-crystalline Fe-Pd alloy, which undergoes a continuous structural transformation. Its superelastic behavior shows near-zero hysteresis, which can be a great advantage due to smaller irreversibility losses; however, its eCE is limited to about 2 K in the temperature range between 240 and 280 K. Furthermore, Guyomar *et al.*²⁵ analyzed the eCE in natural rubber (ASTM D200 AA), which is a shape memory polymer and measured the adiabatic temperature change of 10 K when the sample was elongated for 70% at room temperature (297 K).

Although the eCE has been recognized as a potential cooling mechanism, there is still a lack of knowledge in

designing practical cooling devices. Some demonstration devices have been designed,^{26,27} and as explained by Moya *et al.*⁹ also tested by researchers at the University of Maryland. Furthermore, according to the report of the US Department of Energy²⁸ on the alternative cooling technologies from 2014, the elastocaloric cooling shows the largest potential among all alternative non-vapor-compression HVAC technologies.

The goal of this work is to analyze the eCE of Ni-Ti wires for its possible usage in a practical elastocaloric cooling device around room temperature. Recently performed studies^{5,18–25} on the eCE show a promising potential for its application in a room temperature refrigerator (or heat pump). However, more detailed studies are needed to evaluate its actual potential. The first step in this direction is to analyze the eCE over a wider temperature range (e.g., 30 K which is required for almost all practical applications) together with the associated irreversibilities (the difference between positive and negative adiabatic temperature change) and the impact of the maximum applied strain on the eCE, which are the main goals of this work. These material properties are crucial to how a particular elastocaloric material will perform in an elastocaloric cooling device and are not yet sufficiently addressed in the literature.

II. EXPERIMENTAL

Initially, the Ni-Ti wires were subjected to 400 loading/unloading cycles in order to get a stabilized superelastic response (see Refs. 29–32 for details on the stabilization effect). The trained samples with good functional stability were further tested at two different strain-rates: at low strain-rate (isothermal conditions) and at high strain-rate (adiabatic conditions) at four different temperatures (from 312 K to 342 K with the step of 10 K). At high strain-rate, the adiabatic temperature changes were directly measured using thermocouples. The temperatures were also measured during the training and the isothermal tests in order to verify the assumption of the isothermal conditions. Furthermore, we also analyzed the impact of the maximum applied strain on the adiabatic temperature changes and, by applying an IR camera, also the position and homogeneity of the eCE distribution over the wire during loading.

The tested samples were commercial poly-crystalline Ni-Ti wires with the composition of Ni_{48.9}Ti_{51.1} and the austenitic finish temperature (T_{Af}) around room temperature (≈ 295 K). The samples were 80 mm long with a diameter of 0.7 mm. All the tests were performed under tension loading. The tests (except those using the IR camera) were performed in a thermostatic chamber with the Instron 8874 axial servo-hydraulic testing system and the Dynacell load cell (± 1 kN). The experimental set-up is shown in Fig. 2. The strain was measured with the dynamic mechanical extensometer Instron (with a gage length of 10 mm and range of ± 1 mm), while the temperature was measured by means of two thin thermocouples (type E), with a wire diameter of 0.13 mm mounted on the samples using high-conductivity thermal paste in order to reduce the thermal time constant as much as possible and capture fast temperature changes. Due to speed

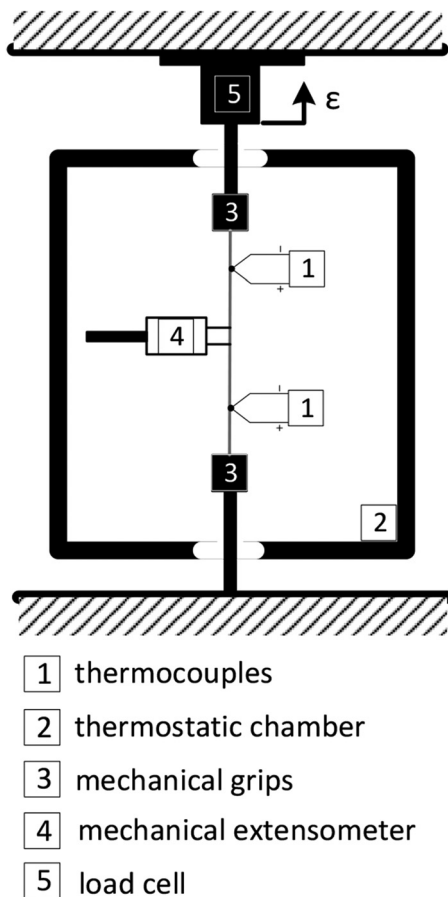


FIG. 2. Schematic show of the experimental set-up.

of the measurements, the sampling frequency of the thermocouples was as high as 80 Hz. In order to analyze the distribution and the homogeneity of the eCE along the sample, we also performed some room temperature tests with the IR camera (FLIR X6540sc) with a frame-rate of 290 fps.

III. RESULTS AND DISCUSSION

A. The training impact

It is well known that during the cycling loading of polycrystalline Ni-Ti alloy, its superelastic behavior degrades, but the effect reaches a steady response after a certain number of cycles. In order to get repeatable results and functional stability, it is therefore crucial to “train” the sample until it reaches the stabilized superelastic behavior before further tests are performed. As explained by various authors, the following is observed during cyclical loading of a virgin (non-trained) sample:^{29–32}

- (1) The critical stress of the transformation plateau associated with the loading (the forward transformation) and unloading (the reverse transformation) decreases with cycling loading.
- (2) The hysteresis area decreases because the decrease of the loading plateau is greater than the unloading plateau.
- (3) The initially flat transformation plateau takes on an increasingly positive slope after a certain number of cycles.

- (4) Gradual increase of irreversible strain and consequential decrease of the transformation strain.
- (5) The training impacts are most pronounced during the initial cycles and tend to be significantly lower after a certain number of cycles.
- (6) The training effects are more pronounced at higher temperatures (due to higher stresses required for transformation).

These training effects and the stabilization of the superelastic behavior in general strongly depend on the material composition, thermal treatment prior cycling, deformation history, texture, grain size, and temperature.³² According to Miyazaki *et al.*,²⁹ the cause for these training degradations is the occurrence of the slip deformation of the crystals during the preceding deformation (at the previous cycle). The internal stress formed by these slip deformations results in residual (locked-in) martensite in the unloaded state and assists the formation of the stress-induced martensite during loading in the next cycle. Therefore, the critical applied stress to induce the transformation decreases. Since the internal stress field (from the previous cycles) has a gradient in its strength, the applied stress for inducing the martensite increases with increasing strain at the transformation plateau. As a result, the transformation plateau is not flat anymore, but rather sloped with smoother transformation knees (also known as the work-hardened superelasticity) as seen in Fig. 3. The degradation becomes insensitive to the cyclic loading after a certain number of cycles (i.e., steady state superelasticity) when no additional slip deformation occurs. Different studies showed approaching a stable level between 100 and 400 cycles.³¹ It should be further noted that the superelastic functional stability is only obtained within a limited temperature range, namely, above the austenitic finish temperature (T_{Af}), which is a precondition for reversible superelasticity and below the certain temperature at which (too) high stress is required for the transformation.³² In the latter case, the residual martensite is widespread throughout the sample (on the account of austenite) and therefore the martensite transformation does not take place anymore.

Figure 3 shows the superelastic behaviors during the training of the Ni-Ti wires at two different temperatures (312 K and 332 K). The same training was applied also at 322 K and 342 K, but since the results have the same trend of dependency, they are not shown here. The wires were subjected to 400 loading/unloading cycles with the strain-rate of 0.001 s^{-1} between 5 N ($\approx 13 \text{ MPa}$) and above the stress required to finish the transformation (the end of the transformation plateau) in the first training cycle at the particular temperature. It is evident that the results shown in Fig. 3 fully agree with the previously observed training effects described above. Namely, the critical stress of transformation plateau, the hysteresis area, and the transformation strain are decreasing during the cycling. The superelastic behavior is well stabilized after 400 cycles with sufficient functional stability to ensure the reproducibility of the results. It is further evident that the training temperature has an important role on the stabilized superelastic behavior. Training at higher temperatures and stresses results in smaller stabilized

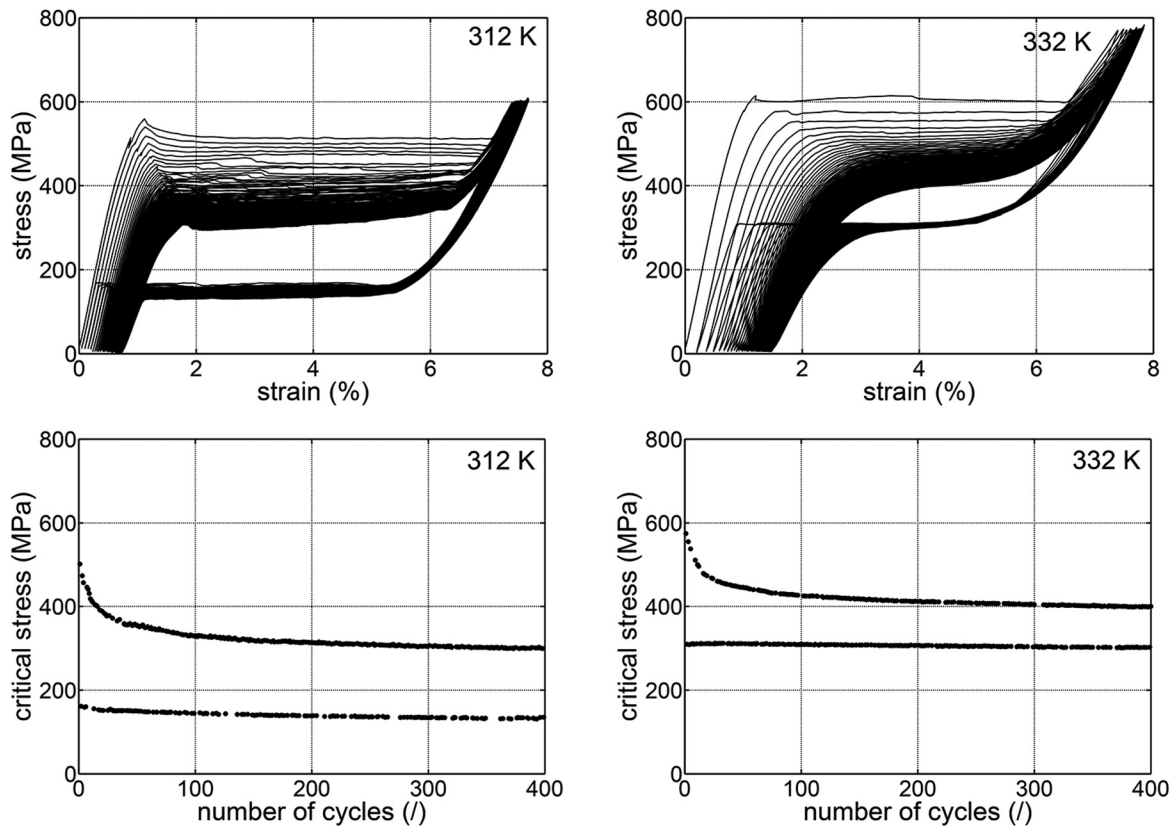


FIG. 3. Up: The superelastic training at two different temperatures. Down: The critical stress at the middle of the transformation plateau as a function of the number of cycles.

transformation strain, smaller hysteresis, and smoother transformation knees compared to the training at lower temperatures (closer to T_{Af}). A direct impact of the training temperature on the eCE is shown and discussed in Sec. III B. It should be mentioned that the strain-rate applied for training causes temperature changes in the wire of about ± 2.5 K (under stable conditions). The chosen strain-rate for the training can influence the stabilization process and the eCE and its impact should be analyzed more in detail in the future.

However, a typical superelastic cycle is as follows (see Fig. 3(up)). Initially, at the low stresses the strain increases almost linearly with the stress (elastic response of the austenitic phase) until the critical transformation stress is reached, where a large (transformation) strain occurs at almost constant stress over the transformation plateau. This corresponds to the stress-induced transformation from the austenitic to the martensitic phase and is associated with the released latent heat. After the transformation is completed, the material further elastically deforms in the martensitic phase. Upon unloading an analogous response occurs, where the strain is recovered with a hysteresis at the transition region.

B. The eCE of the samples trained at different temperatures

The stabilized wires at all four evaluated temperatures were further tested isothermally (at the strain-rate of 0.0002 s^{-1}) and adiabatically (at the strain-rate of 0.2 s^{-1}) at the temperatures at which the wires were trained. The

isothermal strain-rate was defined according to Churchill *et al.*,³³ who suggested that isothermal tests in air should be performed with the strain-rate 0.0004 s^{-1} or less. At the strain-rate applied for the isothermal tests, the temperature changes of the wire did not exceed ± 1 K, which is small enough to be considered isothermal. On the other hand, Vives *et al.*¹⁹ and Ossmer *et al.*²² showed that adiabatic conditions (in air) are well approached with a strain-rate of 0.2 s^{-1} or higher. The measured isothermal and adiabatic superelastic responses of the stabilized wires are shown in Figs. 4 and 5 at four different evaluated temperatures. In the case of isothermal tests, the wires were (un)loaded between 13 MPa and the stress-limit applied at the training (different for each particular temperature). On the other hand, the adiabatic tests were performed with the applied strain limits between the zero strain and the strain, which corresponds to the stress level applied in the isothermal measurements and training (at the particular temperature). The reason for the latter is that the device can overshoot the desired stress when the strain-rate is very high. Due to the self-heating and self-cooling (eCE) of the samples at adiabatic conditions, we hold the samples for 60 s at both final positions in order to reach the ambient temperature. As seen in Fig. 4, the stress drops during that time in the loaded wire due to cooling (natural convection) of the sample at constant strain. This indicates that the transformation was not yet fully completed after loading.

The difference between the superelastic behaviors in the case of isothermal and adiabatic test is clearly seen from

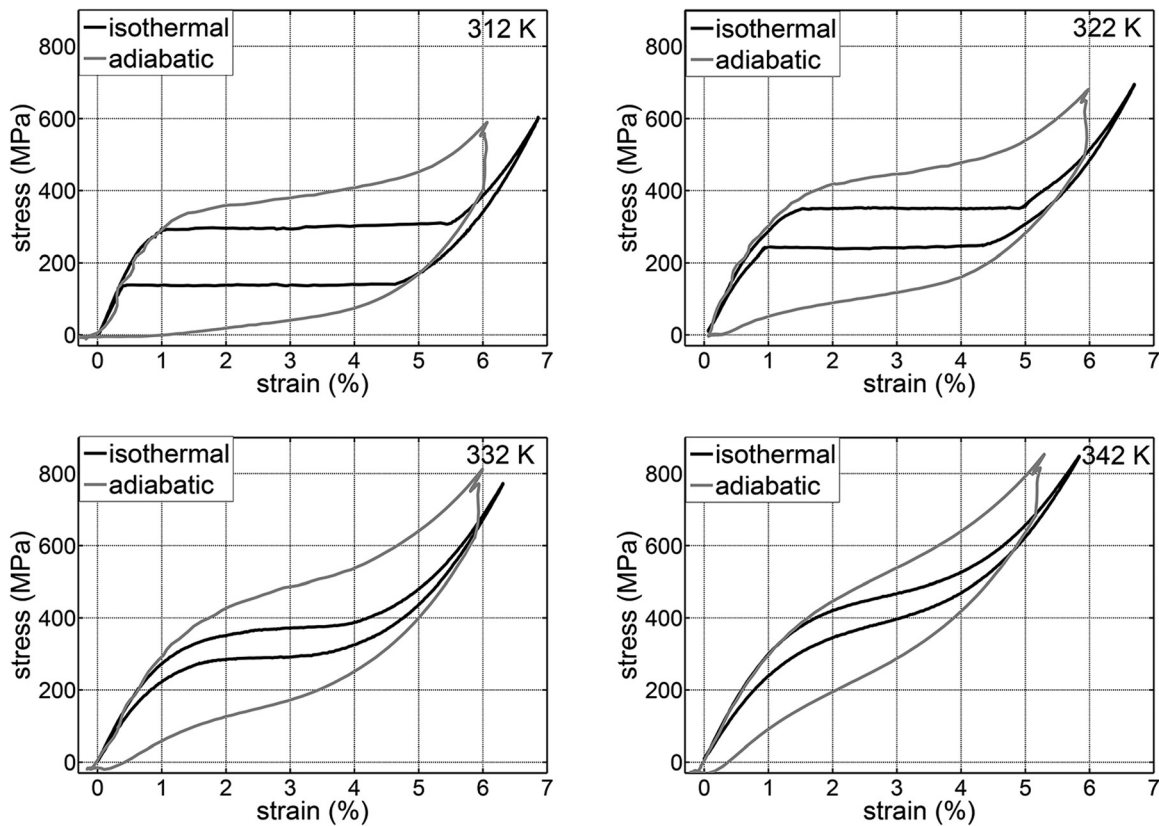


FIG. 4. A comparison of the isothermal (strain-rate of 0.0002 s^{-1}) and adiabatic (strain-rate of 0.2 s^{-1}) superelastic behavior of the stabilized Ni-Ti wires at four different temperatures.

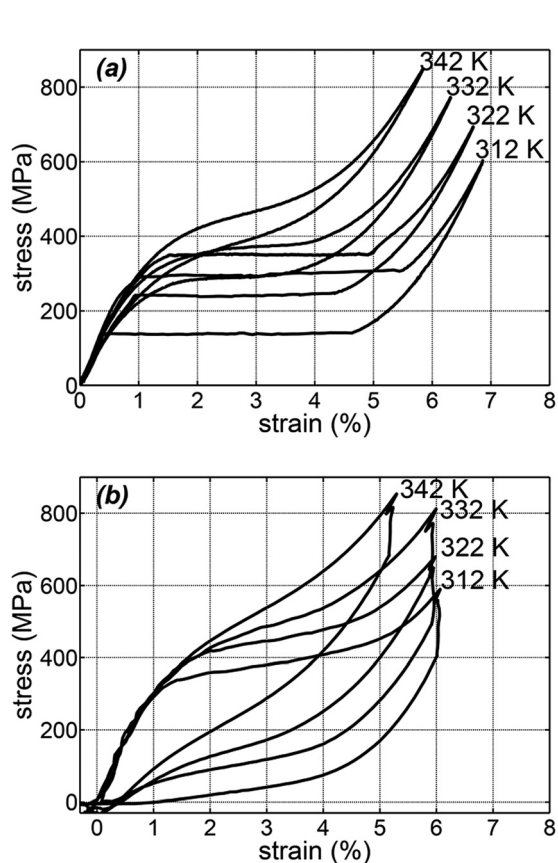


FIG. 5. A direct comparison of temperature dependence of the isothermal (a) and adiabatic (b) superelastic behavior of the stabilized Ni-Ti wires.

Fig. 4. As also explained in the literature,^{14,30,34} the high strain-rates (adiabatic conditions) cause a self-heating (cooling) of the sample, which results in a higher slope of the transformation plateau. In Fig. 5, the impact of the training temperature is evident. As already explained in Sec. III A, the impact of the training is more pronounced at higher temperatures due to the higher stress needed to induce the transformation. This results in smaller hysteresis, smaller transformation strain, and larger slope of the transformation plateau at higher temperatures. However, the elastic modulus in austenitic and martensitic phase remains unchanged (not affected by the training temperature).

Figure 6(a) shows an example of the temperature variations during the adiabatic tests of the wire trained at 342 K. The same tests were performed also at different temperatures and the results are collected in Fig. 6(b).

Figure 6(b) shows the positive adiabatic temperature change (during loading) and negative adiabatic temperature change (during unloading). It should be noted that all the adiabatic tests were performed for 10 successive cycles (with fully reversible superelastic behavior) and the temperature was measured with two thermocouples placed at different parts of the wire (see Fig. 2). Figure 6(b) therefore shows the average adiabatic temperature change of all 10 cycles for both thermocouples, while the error bars show the standard deviation of the measurements. Figure 6(b) also shows the adiabatic temperature changes of the wire trained at 342 K and further adiabatically tested at lower temperatures as explained and shown in Sec. III C. However, in the case of

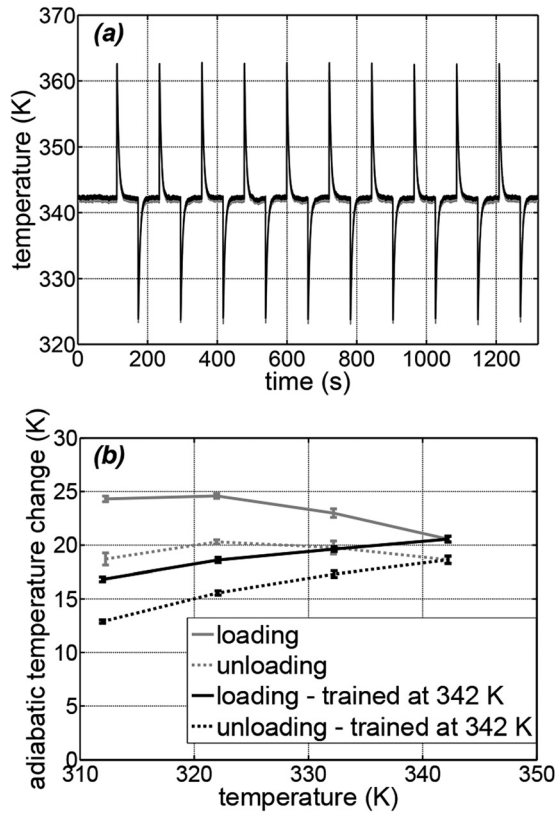


FIG. 6. The temperature variations of both thermocouples during the adiabatic testing at 342 K (a). The adiabatic temperature changes during loading and unloading as a function of temperature at the temperatures at which the wires were trained and for the wire trained at 342 K and tested at lower temperatures, respectively (b).

the wires trained separately at each evaluated temperature, the adiabatic temperature change is increasing with the temperature to the temperatures of about 322 K (where the largest positive adiabatic temperature change is around 25 K and the largest negative one around 21 K). At the temperatures above 332 K, both positive and negative adiabatic temperature changes start to decrease, which is due to the more pronounced training impacts at higher temperatures, namely, smaller transformation strains which directly results in smaller eCE (see Eq. (2)).

The adiabatic temperature changes presented in Fig. 6(b) were not obtained for constant applied stress nor strain change as usually presented for magnetocaloric effect with the constant applied magnetic field change (see Refs. 1–3 for details). Our goal was to apply the stress (or strain) changes required to complete the transformation (to a certain amount) at each particular evaluated temperature. Since the critical stress and strain required for the transformation increase with temperature, the applied stress and strain were therefore increased as well. It should be noted that the transformation is not fully completed at the end of the usually quite well defined plateau, since some, although minor continuing transformation takes place in some parts of the wire even beyond it.³⁵ Strictly speaking, the transformation does not occur exclusively during the stress plateau, but some transformations occur also just before and after the plateau, which are responsible for nonlinearities (smooth transformation

knees) observed at both ends of the plateau.³³ In order to perform equal level of transformation at each temperature, a stress of approximately 200 MPa above the stress level associated with the end of the transformation plateau was applied at each temperature (see Fig. 5(a)).

One should note that there are two types of heat sources that result in the adiabatic temperature change, the latent heat of the phase transformation (eCE) and intrinsic mechanical dissipative heat of internal friction (seen in the hysteresis), respectively.³⁶ The latter causes an entropy generation, which results in increased adiabatic temperature change during loading and decreased adiabatic temperature change during unloading. Here, it is assumed that the entire dissipative energy due to the hysteresis transforms into heat (and not into sound or other vibrations). Figure 7 shows the measured temperature irreversibilities (the difference between the adiabatic temperature change during loading and unloading shown in Fig. 6(a)) and the irreversibilities calculated based on the hysteresis area (Q_{hyst}) of the isothermal tests. The latter was calculated using the following equation:

$$\Delta T_{irr} = \frac{T}{c} \Delta s_{irr} = \frac{T}{c} \frac{Q_{hyst}}{T} = \frac{1}{\rho c} \oint (\sigma \cdot d\varepsilon), \quad (1)$$

where the density (ρ) is 6500 kg/m³ and the specific heat (c) is estimated to 450 J/kg K.³⁷ It should be noted that the irreversible entropy generation is obtained from the hysteresis area of the isothermal tests since the adiabatic hysteresis additionally includes the thermodynamic work needed to perform the cooling cycle with self-heating and self-cooling of the material. This is also clearly seen by comparing the isothermal and adiabatic tests in Fig. 4. Figure 7 also shows the temperature irreversibilities of the wire trained at 342 K and further adiabatically tested at lower temperatures as explained in Sec. III C. However, in the case of separately trained wires it is evident that the measured as well as the calculated temperature irreversibilities are decreasing with temperatures. Such a trend was expected, since the hysteresis area is decreasing with temperatures as well (see Figs. 4 and 5). Comparing the measured and calculated temperature irreversibilities, it can be concluded that there is another source of the irreversibilities. This can be attributed to some

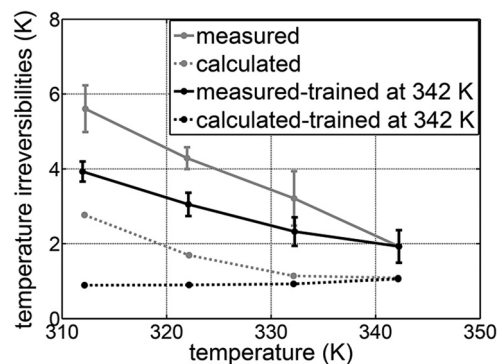


FIG. 7. The measured and calculated temperature irreversibilities at the temperatures at which the wires were trained and for the wire trained at 342 K and tested at lower temperatures, respectively.

temporary residual strain as also explained in Ref. 38. When the wire is adiabatically unloaded (with self-cooling), the reverse transformation remains incomplete with residual strain (martensite) when the zero stress is reached (see Fig. 5(b)). That means that the martensite is not fully transformed back to austenite and as a result a slight bending of the wire occurs. The strain is self-recovered afterwards and the wire is straightened as it is heated back to ambient temperature, which causes the remainder of the martensite to transform to austenite. Full reversibility of the superelastic reverse transformation is therefore limited and the related negative adiabatic temperature change is reduced. As seen in Fig. 5(b), this is more pronounced at lower temperatures, as at higher temperatures the plateaus occur at higher stresses and the transformation can be more completed when the zero stress is reached. This shows that in order to reduce the irreversibilities (and increase the performance of the potential cooling device) this particular wire should be applied at the temperatures well above its austenitic finish temperature (T_{Af}) or better, the materials with more completed reverse transformation after the unloading should be applied. The latter can be potentially achieved by reducing the training effects, such as work-hardening and smoothing of the transformation knees, which can be accomplished by special heat treatment prior to the loading cycling and can result in much less sensitive superelastic behavior against cycling deformation—see Refs. 29 and 39. The level of the incomplete transformation after unloading can also be reduced by increasing the heat transfer between the specimen and ambient, which can potentially lead to isothermal (un)loading that is utilized in, for example, an Ericsson-like thermodynamic cycle. However, one should distinguish between both sources of the irreversibilities and its impact on the elastocaloric cooling device. The irreversible entropy generation due to the hysteresis results in additional input work to perform the elastocaloric thermodynamic cycle (increasing the heating power and decreasing the cooling power of the potential device). On the other hand, the irreversibilities due to the temporary residual strain disable the utilization of the available latent heat of the reverse transformation, thus decreasing the cooling power of the potential elastocaloric device, but do not significantly influence the input work into the thermodynamic cycle.

If one compares the temperature irreversibilities obtained in this work, with the previously published values^{5,22} in Ni-Ti alloy the following conclusion can be made. In Cui *et al.*,⁵ the temperature irreversibilities of above 8 K were measured in the Ni-Ti wire, while in Ossmer *et al.*²² the temperature irreversibilities of 1 K were measured in the Ni-Ti thin film. Since both areas of the stress-strain hysteresis are relatively similar, it can be concluded that in the Ni-Ti wire analyzed by Cui *et al.*⁵ the temporary residual strain (or even irreversible strain) after the unloading was significantly larger compared to the Ni-Ti thin film analyzed by Ossmer *et al.*²² This can be mainly due to larger difference between the austenitic finish temperature and the testing temperature in experiment performed by Ossmer *et al.*²² compared to the experiment performed by Cui *et al.*,⁵ the

difference in the microstructure between thin film and bulk samples and different history of the samples.

C. The eCE of the samples trained at 342 K

Most practical cooling devices operate at temperature spans between the heat source and the heat sink of approximately 30 K or more. Utilizing the eCE, this can be efficiently accomplished by the application of a regenerative cycle as demonstrated in magnetic refrigeration with the active magnetic regenerator (see Refs. 40 and 41 for details). During the operation of such device, a temperature profile is established along its length which means that each part of the material in the regenerator should be able to work at different temperatures. In order for Ni-Ti wires to be applied in the elastocaloric regenerator, they will have to be able to reproducibly operate over a range of temperatures. However, the wire trained at, e.g., 312 K will change its superelastic response when loaded at higher temperatures and stresses as it was not trained at these stresses. On the other hand, Fig. 8 shows the isothermal and adiabatic superelastic behaviors at four different temperatures of the wire trained at 342 K. Both types of tests were performed the same as for the separately trained wires described in Sec. III B. As shown in Fig. 8(a) and previously also by various authors,^{14,30,35} the isothermal superelastic stress-strain curves of stabilized material at different temperatures fit to the same austenitic and martensitic elastic modulus lines, with the same transformation strain, but different critical stress of the transformation. We can

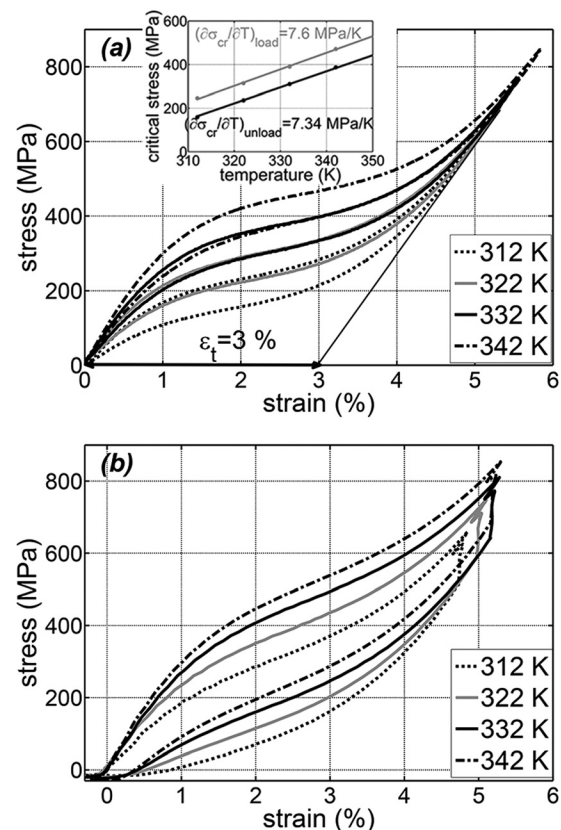


FIG. 8. A comparison of the isothermal (a) and adiabatic (b) superelastic responses of the stabilized Ni-Ti wire trained at 342 K at different temperatures.

therefore conclude that the wire trained at 342 K can be repeatable cyclically loaded also at lower temperatures with no additional degradation of superelastic behavior, which makes it possible to apply it in the elastocaloric regenerator.

The results shown in Fig. 8(a) can be further used to estimate the isothermal entropy change using the Clausius-Clapeyron equation:

$$\Delta s = -\frac{1}{\rho} \varepsilon_t \left(\frac{\partial \sigma_{cr}}{\partial T} \right). \quad (2)$$

According to Fig. 8(a), the transformation strain (ε_t) is 0.03 and the Clausius-Clapeyron factors ($\partial \sigma_{cr} / \partial T$), which present the slope of the critical transformation stress (see inset in Fig. 8(a)) are 7.6 MPa/K for loading and 7.34 MPa/K for unloading. Using Eq. (2), the estimated isothermal entropy change is 35.1 J/kg K for loading and 33.9 J/kg K for unloading over the analyzed temperature range. The difference in entropy changes for loading and unloading represents the irreversible entropy generation due to hysteresis and result directly from the difference in the Clausius-Clapeyron factors of the forward and reverse transformation. It should be noted that the estimated values of the entropy changes assume that a complete transformation was performed, which is due to the fact that some minor transformations usually occur even beyond the plateau, rather hard to achieve in reality.

Figure 8(b) shows the adiabatic superelastic behavior at four different temperatures, while the associated adiabatic temperature changes are shown in Fig. 6(b). As expected according to Manosa *et al.*,²⁰ the adiabatic temperature change is increasing with temperature for the entire analyzed temperature range. Comparing the adiabatic temperature changes of the wires trained separately at lower temperatures and the wire trained at 342 K, we can conclude that in the latter case the sample exhibits smaller eCE, mostly due to smaller transformation strains (comparing Figs. 5 and 8). Furthermore, as shown in Fig. 7 the wire trained at 342 K also shows smaller irreversibilities, which was expected due to smaller hysteresis compared to the wires trained at lower temperatures. However, the calculated temperature irreversibilities due to the hysteresis are slightly increasing with the temperature as the hysteresis areas are increasing as well, while we measured quite larger irreversibilities with the decreasing trend. As already explained is Sec. III B, this is due to the temporary residual strain after the unloading, which is more pronounced at lower temperatures.

D. The impact of the maximum applied strain

We further studied the eCE and its dependence on the maximum applied strain. The wire was trained at the same way as for the previous tests, but to larger maximum stress (in order to be able to evaluate the eCE also at larger strains with the stabilized behavior). As seen in Fig. 9(a), this training causes even less distinctive transformation plateau with smoother transformation knees compared to the previous case when the wire was trained to lower maximum stress (grey line in Fig. 9(a)). As seen from Fig. 9(a), this further

causes larger degree of the temporary residual strain immediately after the unloading and therefore larger temperature irreversibilities. However, Fig. 9 shows the adiabatic superelastic behaviors at 342 K at different maximum applied strains and the related adiabatic temperature changes. It is evident that the positive as well as the negative adiabatic temperature changes are increasing with the increased applied strain, with a kind of inflection point between 4% and 5%, which is related with the end of the transformation plateau (see Fig. 9(a)). It can be concluded that at the strain of 5.5%, the forward transformation is not yet fully completed. It is to be expected that this would occur at even larger strain at which the (positive) adiabatic temperature change will not increase with strain anymore. This is strongly related with the fact that the transformation is not fully completed at the end of the transformation plateau, but some transformations occur even beyond (and before) the plateau, as already explained above. It is also evident from Fig. 9(b) that the temperature irreversibilities are increasing with the increased strain. Namely, both sources of the temperature irreversibilities are increasing with the increased strain, since larger strain results in larger hysteresis as well as in larger degree of the temporary residual strain after unloading (see Fig. 9(a)). It can be concluded that in order to obtain the largest adiabatic temperature change the strains above the transformation plateau should be applied. On the other hand, in order to reduce the input work to perform the cooling cycle and the temperature irreversibilities, as well as

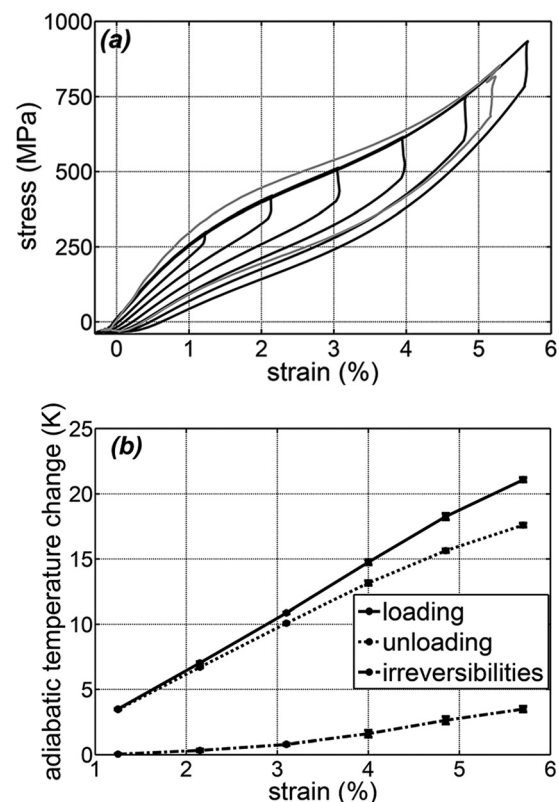


FIG. 9. The adiabatic superelastic responses at different applied strains at 342 K, where the grey line shows the results from Sec. III C (a) and the related adiabatic temperature changes (b).

to potentially increase the fatigue life, it might be beneficial to limit the applied strain to smaller values.

E. The distribution and the homogeneity of the eCE

It is important to know how the eCE and the related adiabatic temperature changes are spatially distributed over the sample during the transformation. This is especially important for application of the elastocaloric material in a practical device, where the homogeneous distribution of the eCE is strongly desirable. As clearly shown by Churchill *et al.*,³³ during uniaxial tensile stress-induced transformation many Ni-Ti alloys have well-known material-level instabilities that result in localized deformation and propagation of transformation fronts (so-called Lüders bands—see Refs. 42 and 43 for details). During low strain-rate transformation (forward and reverse), the transformation occurs by the propagation of usually two boundaries separating nearly uniform high-strain and low-strain regions. However, higher strain-rates result in the nucleation of more fronts as mechanical nucleation barriers are surmounted via the non-uniform temperature fields in the sample. Similar was also shown by Vives *et al.*,¹⁹ who analyzed the temperature contour maps (distribution of the adiabatic temperature changes) in the single-crystalline Cu-Al-Zn alloy using thermography. They showed markedly inhomogeneous temperature profile along the sample, with significant distribution of the adiabatic temperature change.

Figure 10 (Multimedia view) shows the temperature distribution over Ni-Ti wires measured with a FLIR X6540sc IR camera during loading at adiabatic conditions. Here, only one time-segment during the transformation is shown—see "Multimedia view" for the transient temperature response during the entire transformation. Three samples were analyzed; the virgin wire, the wire trained at 312 K, and the wire trained at 342 K. Due to the space limitation in the thermostatic chamber, the measurements were performed at room temperature (around 300 K). Furthermore, since the austenitic finish temperature of this particular material is around room temperature, a significant temporary residual strain occurs during the high strain-rate unloading (and subsequent cooling) at this temperature. This is the reason for analyzing the distribution of the eCE only during loading. However, as shown in Ref. 42 similar behavior is expected for forward and reverse transformation (although with potentially different number of transformation fronts), but in the latter case the transformations first appear at those locations where the previous forward transformation ended.²² It is also important to note that the emissivity of the wires was not well controlled and therefore all IR images do not necessarily represent high accuracy temperature measurements. All IR figures and videos are intended to demonstrate the magnitude and uniformity of the temperature change but were not used to characterize material properties.

Comparing the results shown in Fig. 10 (Multimedia view), we can conclude that the eCE in the virgin wire is nucleated randomly along the wire and shows significant instabilities and transformation fronts (Lüders bands). A similar effect is observed in the wire trained at 312 K but this time the distribution of the nucleation is "spread out" over

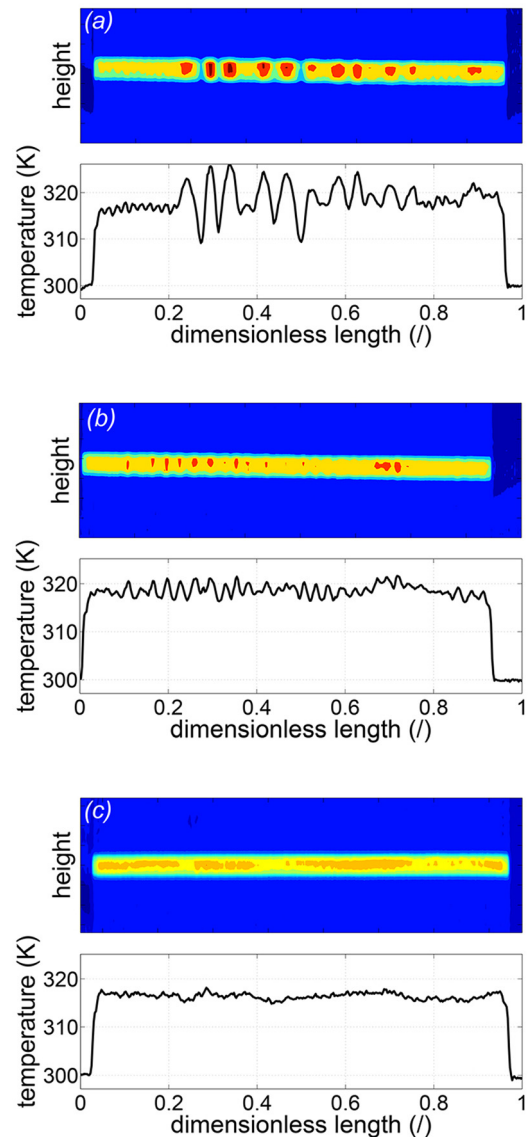


FIG. 10. The distribution of the temperature changes during loading: (a) virgin wire; (b) wire trained at 312 K, and (c) wire trained at 342 K. The emissivity of the Ni-Ti wire was estimated to 0.75.⁴⁵ (Multimedia view) [URL: <http://dx.doi.org/10.1063/1.4913878.1>] [URL: <http://dx.doi.org/10.1063/1.4913878.2>] [URL: <http://dx.doi.org/10.1063/1.4913878.3>]

the whole sample, while the eCE is almost completely homogeneous in the wire trained at 342 K without any possibility to identify where the nucleation starts. The different nature of the transformation, which results from different training conditions, is related to the superelastic behavior at the transformation plateau. The localized, Lüders-like transformation fronts are observed at the flat transformation plateau, while they become diffuse and no longer discernible when the plateau takes on a positive slope in the trained samples.^{43,44} Due to similar transformation plateaus during loading and unloading at the particular temperature and training conditions (see Figs. 5 and 8), one can therefore expect similar nature of the transformation as observed during loading also during unloading (with significant instabilities in the case of virgin wire and almost completely homogeneous eCE in the case of the wire trained at 342 K). However, this should be evaluated and analyzed in the future. As expected, the

adiabatic temperature change in the virgin sample is higher compared to the trained ones.

IV. CONCLUSION

A detailed study of the superelastic behavior and the related eCE of the Ni-Ti wire was conducted at different temperatures. The wires were initially trained to stabilize the superelastic behavior and to ensure the reproducible operation. The stabilized wires were further tested isothermally (strain-rate of 0.0002 s^{-1}) and adiabatically (strain-rate of 0.2 s^{-1}) to measure the adiabatic temperature changes. It was shown that the training temperature has an important impact on the eCE. Higher the training temperature is larger the degradation of the superelastic behavior will be, which reduces the eCE as well as the associated irreversibilities. The largest adiabatic temperature change was measured at around 322 K (also trained at this temperature), where the wire heats up for about 25 K during loading and cools down for about 21 K during unloading. For the wire trained at 342 K and adiabatically tested at lower temperatures, which will be the case also in the practical elastocaloric regenerator-based cooling device, the positive adiabatic temperature changes are between 17 K (at 312 K) and 21 K (at 342 K) and the negative adiabatic temperature changes are between 13 K (at 312 K) and 19 K (at 342 K). The estimated isothermal entropy changes using the Clausius-Clapeyron equation are 35.1 J/kg K for loading and 33.9 J/kg K for unloading, respectively. It was shown that there are two sources of the temperature irreversibilities, the hysteresis (and related entropy generation) and the occurrences of the temporary residual strain, which decreases the adiabatic temperature change during the unloading especially at lower temperatures (closer to T_{Af}).

We further analyzed the impact of the maximum applied strain on the adiabatic temperature changes. It was shown that both the positive and the negative adiabatic temperature changes are increasing with the applied strain (for the analyzed strain range) and the temperature irreversibilities are increasing as well. With the increased applied strain, both sources of the temperature irreversibilities (the entropy generation due to hysteresis and the temporary residual strain) are increasing. It should be noted that with the maximum applied strain we have not yet reached the complete martensitic transformation, which would occur at even larger strains (where the adiabatic temperature change would not increase with strain anymore).

We also evaluated the homogeneity and the distribution of the eCE and the related adiabatic temperature changes over the wire during loading using the IR camera. It was concluded that the virgin wire exhibits significant instabilities and highly nonhomogeneous distribution of the eCE during loading, while with training (especially at higher temperatures—well above the T_{Af}) the eCE becomes diffuse and highly uniform. The latter is preferable for the application of the Ni-Ti wire in the cooling device.

If one compares the eCE of the Ni-Ti wire with other caloric effects, especially the magnetocaloric effect which is up-to-date the most widely analyzed for its application in the

future environmental-friendly solid-state cooling device, it can be concluded that the elastocaloric adiabatic temperature changes are significantly larger. The best magnetocaloric materials in the magnetic fields accessible with the permanent magnets (up to 1.5 T) only have the adiabatic temperature change up to 5 K and in much narrower temperature range compared to the eCE (see Refs. 9 and 20 for detailed comparison). The eCE therefore shows a large potential to be applied in the cooling (or heat-pumping) device. However, beside the large eCE the following is required in order the elastocaloric material to be implemented in the real (and efficient) device, which is our final goal

- (1) Both sources of the irreversibilities, the hysteresis (which decreases the efficiency of the device) and the temporary residual strain after the unloading (which decreases the negative adiabatic temperature change and therefore the cooling power of the device) should be reduced as much as possible. This will have to be evaluated through the numerical modeling of the potential cooling device in the future. Bending of the sample during unloading associated with the temporary residual strain presents also a serious issue for the operation of the device and should be avoided.
- (2) Materials with suitable transformation temperatures. In particular, the austenitic finish temperature should be around but lower than the refrigeration temperature (to avoid any non-recoverable strain). The material evaluated in this work can be applied in cooling applications with the refrigeration temperature above 310 K (but the knowledge obtained with this material can be analogously applied also for materials with lower transformation temperatures at lower and more suitable temperatures for wider cooling applications). At the same time, the austenitic finish temperature should not be too low in order to avoid high stresses to perform the transformation.
- (3) Long fatigue life and good functional stability. This is currently the main limitation of this technology. The elastocaloric materials to be implemented in the cooling device will have to be able to perform up to 10^8 cycles (in the life time of 10 yr). This is currently still not achievable; however, the latest results⁴⁶ on Ni-Ti thin films doped with Cu and Co are very promising and show no fatigue and good functional stability even after 10^6 cycles. This is an important step forward in the development of the applicable elastocaloric materials.

ACKNOWLEDGMENTS

J.T. wishes to thank DTU's international H.C. Ørsted postdoc program for supporting this work.

¹S. Fähler, U. K. Röbber, O. Kastner, J. Eckert, G. Eggeler, H. Emmerich, P. Entel, S. Müller, E. Quandt, and K. Albe, *Adv. Eng. Mater.* **14**, 10–19 (2012).

²A. M. Tishin and Y. I. Spichkin, *The Magnetocaloric Effect and its Application* (Institute of Physics Publishing, Bristol, United Kingdom, 2003).

³K. G. Sandeman, *Scr. Mater.* **67**, 566–571 (2012).

- ⁴A. Smith, C. R. H. Bahl, R. Bjørk, K. Engelbrecht, K. K. Nielsen, and N. Pryds, *Adv. Energy Mater.* **2**, 1288–1318 (2012).
- ⁵J. Cui, Y. Wu, J. Muehlbauer, Y. Hwang, R. Radermacher, S. Fackle, M. Wuttig, and I. Takeuchi, *Appl. Phys. Lett.* **101**, 073904 (2012).
- ⁶J. A. Shaw, C. B. Churchill, and M. A. Iadicola, *Exp. Tech.* **32**, 55–62 (2008).
- ⁷*Shape Memory Materials*, edited by K. Otsuka and C. M. Wayman (Cambridge University Press, Cambridge, 1998).
- ⁸C. Liu, H. Qin, and P. T. Mather, *J. Mater. Chem.* **17**, 1543–1558 (2007).
- ⁹X. Moya, S. Kar-Narayan, and N. D. Mathur, *Nature Mater.* **13**, 439–450 (2014).
- ¹⁰C. Rodriguez and L. C. Brown, *Metall. Trans. A* **11**, 147–150 (1980).
- ¹¹L. C. Brown, *Metall. Trans. A* **12**, 1491–1494 (1981).
- ¹²K. Mukherjee, S. Sircar, and N. B. Dahotre, *Mater. Sci. Eng.* **74**, 75–84 (1985).
- ¹³P. G. McCormick, Y. Liu, and S. Miyazaki, *Mater. Sci. Eng., A* **167**, 51–56 (1993).
- ¹⁴C. B. Churchill, J. A. Shaw, and M. A. Iadicola, *Exp. Tech.* **34**, 63–80 (2010).
- ¹⁵E. Pieczyska, *J. Mod. Opt.* **57**, 1700–1707 (2010).
- ¹⁶H. Yin, Y. He, and Q. Sun, *J. Mech. Phys. Solids* **67**, 100–128 (2014).
- ¹⁷S. A. Nikitin, G. Myalikgulyev, M. P. Annaorazov, A. L. Tyurin, R. W. Myndyev, and S. A. Akopyan, *Phys. Lett. A* **171**, 234–236 (1992).
- ¹⁸E. Bonnot, R. Romero, L. Manosa, E. Vives, and A. Planes, *Phys. Rev. Lett.* **100**, 125901 (2008).
- ¹⁹E. Vives, S. Burrows, R. S. Edwards, S. Dixon, L. Manosa, A. Planes, and R. Romero, *Appl. Phys. Lett.* **98**, 011902 (2011).
- ²⁰L. Manosa, S. Jarque-Farnos, E. Vives, and A. Planes, *Appl. Phys. Lett.* **103**, 211904 (2013).
- ²¹H. Ossmer, C. Chluba, B. Krevet, E. Quandt, M. Rohde, and M. Kohl, *J. Phys.: Conf. Ser.* **476**, 012138 (2013).
- ²²H. Ossmer, F. Lambrecht, M. Gultig, C. Chluba, E. Quandt, and M. Kohl, *Acta Mater.* **81**, 9–20 (2014).
- ²³C. Bechtold, C. Chluba, R. Lima de Miranda, and E. Quandt, *Appl. Phys. Lett.* **101**, 091903 (2012).
- ²⁴F. Xiao, T. Fukuda, and T. Kakeshita, *Appl. Phys. Lett.* **102**, 161914 (2013).
- ²⁵D. Guyomar, Y. Li, G. Sebald, P. J. Cottinet, B. Ducharme, and J. F. Capsal, *Appl. Therm. Eng.* **57**, 33–38 (2013).
- ²⁶A. J. DeGregoria, International patent WO 94/10517 (11 May 1994).
- ²⁷J. Cui, I. Takeuchi, M. Wuttig, Y. Wu, R. Radermacher, Y. Hwang, and J. Muehlbauer, U.S. patent application US 2012/0273158 A1 (1 November 2012).
- ²⁸W. Goetzler, R. Zogg, J. Young, and C. Johnson, *Energy Savings Potential and RD&D Opportunities for Non-Vapor-Compression HVAC Technologies*, prepared for U.S. Department of Energy (Navigant Consulting, Inc., 2014).
- ²⁹S. Miyazaki, T. Imai, Y. Igo, and K. Otsuka, *Metall. Trans. A* **17**, 115–120 (1986).
- ³⁰H. Tobushi, Y. Shimeno, T. Hachisuka, and K. Tanaka, *Mech. Mater.* **30**, 141–150 (1998).
- ³¹I. Schmidt and R. Lammerling, *Z. Angew. Math. Mech.* **80**, 453–454 (2000).
- ³²J. Olbricht, A. Yawny, A. M. Condo, F. C. Lovey, and G. Eggeler, *Mater. Sci. Eng., A* **481–482**, 142–145 (2008).
- ³³C. B. Churchill, J. A. Shaw, and M. A. Iadicola, *Exp. Tech.* **33**, 51–62 (2009).
- ³⁴I. Schmidt, *J. Eng. Mater. - Trans. ASME* **128**, 279–284 (2006).
- ³⁵Y. Liu, A. Mahmud, F. Kursawe, and T. H. Nam, *J. Alloys Compd.* **449**, 82–87 (2008).
- ³⁶J. Ortin and A. Planes, *Acta Metall.* **37**, 1433–1441 (1989).
- ³⁷C. Zanotti, P. Giuliani, and A. Chrysanthou, *Intermetallics* **24**, 106–114 (2012).
- ³⁸W. W. Chen, Q. P. Wu, J. H. Kang, and N. A. Winfree, *Int. J. Solids Struct.* **38**, 8989–8998 (2001).
- ³⁹B. Erbstoeszer, B. Armstrong, M. Taya, and K. Inoue, *Scr. Mater.* **42**, 1145–1150 (2000).
- ⁴⁰J. Tušek, A. Kitanovski, S. Zupan, I. Prebil, and A. Poredoš, *Appl. Therm. Eng.* **53**, 57–66 (2013).
- ⁴¹K. Engelbrecht, D. Eriksen, C. R. H. Bahl, R. Bjørk, J. Geyti, J. A. Lozano, K. K. Nielsen, F. Saxild, A. Smith, and N. Pryds, *Int. J. Refrig.* **35**, 1498–1505 (2012).
- ⁴²C. B. Churchill, J. A. Shaw, and M. A. Iadicola, *Exp. Tech.* **33**, 70–78 (2009).
- ⁴³P. Sittner, Y. Liu, and V. Novak, *J. Mech. Phys. Solids* **53**, 1719–1746 (2005).
- ⁴⁴Y. Liu, I. Houver, H. Xiang, L. Bataillard, and S. Miyazaki, *Metall. Mater. Trans. A* **30**, 1275–1282 (1999).
- ⁴⁵J. Zurbitu, S. Kustov, A. Zabaleta, E. Cesari, and J. Aurrekoetxea, “Thermo-mechanical behaviour of NiTi at impact,” in *Shape Memory Alloys*, edited by C. Cismasiu (InTech, 2010).
- ⁴⁶C. Chluba, R. Lima-de-Miranda, L. Kienle, M. Wuttig, A. Khachatryan, and E. Quandt, Oral presentation at the International Conference on Martensitic Transformation (ICOMAT), Bilbao, Spain, 6 July–11 July 2014.